Particle bound Reactive Oxygen Species emitted from indoor sources – assessment through offline methods

Fredric Ahrling

DIVISION OF ERGONOMICS AND AEROSOL TECHNOLOGY | DEPARTMENT OF DESIGN SCIENCES
FACULTY OF ENGINEERING LTH | LUND UNIVERSITY
2026

MASTER THESIS

Particle bound Reactive Oxygen Species emitted from indoor sources

assessment through offline methods

Fredric Ahrling

LUND
UNIVERSITY

Particle bound Reactive Oxygen Species emitted from indoor sources

Assessment through offline methods

Published by
Department of Design Sciences
Faculty of Engineering LTH, Lund University
P.O. Box 118, SE-221 00 Lund, Sweden

Subject: Aerosol Technology (MAMM05)
Division: Ergonomics and Aerosol Technology
Supervisor: Aneta Wierzbicka
Co-supervisor: Jonas Enarsson
Examiner: Malin Alsved

Abstract

Particle-bound reactive oxygen species (ROS) play a key role in mechanisms linking particulate air pollution to adverse health effects through oxidative stress. Understanding the ways in which humans are exposed to ROS is important, and since humans spend most of their time indoors, indoor air quality is a relevant field of research. This thesis investigates particle-bound ROS emitted from typical household activities using offline analytical methods and compares the results with data from a novel online measurement technique, the Particle Into Nitroxide Quencher (PINQ).

Particles were generated in an aerosol chamber from several indoor sources, including candle burning, incense, frying, secondary organic aerosol (SOA) formation from air fresheners, and squalene-ozone reactions representing human skin reacting with ozone, as well as combinations of these sources. Particles were collected on filters and extracted for offline ROS analysis using the dichlorofluorescein (DCFH) assay and spectrofluorometry. The results were compared with real-time ROS measurements during generation obtained using the PINQ, which employs the BPEAnit probe. Additional particle characterization data, including particle size, black carbon concentration, and metal content, were analyzed to explore potential relationships with ROS levels.

The offline method detected particle-bound ROS in all sampled particle types, with particularly high levels observed for candle- and incense-related emissions. However, large variability was found between experiments of the same particle type. Online PINQ measurements showed both positive and negative ROS signals, likely influenced by probe sensitivity and scavenging effects from black carbon. Comparisons between methods reveal limited agreement, highlighting differences in chemical sensitivity, temporal resolution, and methodological constraints.

The results demonstrate that ROS is present on particles in indoor air, hence their health effects are of relevance for further assessment. However, the complexity of assessing particle-bound ROS suggests that no single method can fully capture the oxidative properties of indoor aerosols.

Keywords: Reactive oxygen species, indoor air quality, particulate matter, aerosol technology, Particle Into Nitroxide Quencher (PINQ)

Sammanfattning

Partikelbundna reaktiva syreföreningar (ROS) spelar en central roll i mekanismer som kopplar luftföroreningspartiklar till negativa hälsoeffekter genom oxidativ stress. Förståelsen för hur människor exponeras för ROS är därför viktig och eftersom människor tillbringar större delen av sin tid inomhus är inomhusluftens kvalitet ett relevant forskningsområde. Denna examensuppsats undersöker partikelbunda ROS som avges vid typiska hushållsaktiviteter med hjälp av offline analytiska metoder och jämför resultaten med data från en ny online-mätteknik, Particle Into Nitroxide Quencher (PINQ).

Partiklar genererades i en aerosolkammare från flera inomhuskällor. Dessa inkluderar stearinljus, rökelse, stekning, bildning av sekundära organiska aerosoler (SOA) från luftfräschare samt reaktioner mellan squalen (som representerar hud) och ozon, både var för sig och i kombinationer. Partiklar samlades på filter och extraherades för offline-analys av ROS med hjälp av diklorofluorescein (DCFH) som kemisk prob och spektrofluorometri. Resultaten jämfördes med realtidsmätningar av ROS utförda med PINQ-instrumentet, som använder den kemiska proben BPEAnit. Ytterligare partikelkarakterisering, inklusive partikelstorlek, halt av svart kol och metallinnehåll, analyserades för att undersöka potentiella samband med ROS-nivåer.

Offline-metoden detekterade partikelbundna ROS i samtliga undersökta partikeltyper, med särskilt höga nivåer för emissioner relaterade till stearinljus och rökelse. Samtidigt observerades betydande variationer mellan experiment av samma partikeltyp. Online-mätningar med PINQ uppvisade både positiva och negativa ROS-signaler, vilket sannolikt påverkades av probens känslighet samt scavenging-effekter från svart kol. Jämförelser mellan metoderna visar begränsad överensstämmelse, vilket belyser skillnader i kemisk känslighet, tidsupplösning och metodologiska begränsningar.

Resultaten visar att ROS finns på partiklar i inomhusluft, vilket innebär att det är relevant att fortsatt studera dess hälsoeffekter. Dock indikerar komplexiteten i att bedöma partikelbundna ROS att ingen enskild metod fullt ut kan fånga de oxidativa egenskaperna hos inomhusaerosoler.

Nyckelord: Reaktiva syreföreningar, inomhusluftens kvalitet, luftburna partiklar, aerosolteknologi, Particle Into Nitroxide Quencher (PINQ)

Acknowledgments

I would like to thank my supervisors, Aneta and Jonas, for trusting me with this project and their precious aerosol samples. Their guidance through laboratory work and continuous feedback on this thesis has been invaluable. I would also like to thank everyone at the department who has patiently shared laboratory space, equipment, and insights with me.

Research projects that formed basis for this thesis, were funded by A Swedish Research Council for Sustainable Development, Formas (Dnr 2020-01370), The Swedish Research Council (Dnr 2021-05049) and Nanolund (p09-2021).

Lund, January 2026

Fredric Ahrling

Table of contents

1 Introduction

1.1 Background

The World Health Organization (WHO) reported that in 2019, air pollution carried responsibility for 6.7 million deaths annually, accounting for one eighth of global deaths, making it the largest environmental risk to health (WHO, 2024). Both ambient and household air pollution contributes to mortality. Understanding and monitoring the sources of air pollution is therefore important to improve public health.

Although the exact mechanisms and what types of air pollution contribute to mortality are not completely understood, fine particulate matter (PM) has been named a leading cause, with reactive oxygen species (ROS) likely being behind a majorly contributing mechanism (Chow, et al., 2006; Bates, et al., 2015; Strak, et al., 2012). ROS is a collective term describing oxygen-containing reactive species (Li & Trush, 2016). These include free radicals, gaining their reactiveness from having unpaired electrons, such as superoxide ($O_2^{\cdot-}$). An example of ROS that is not a free radical is hydrogen peroxide (H_2O_2), which has weak oxygen-oxygen bonds.

The mechanism in question is oxidative stress, which occurs when the concentration of ROS exceeds the body's antioxidant ability. This induces a redox state change in cells that can lead to inflammation, chemical altering of DNA, proteins, and lipids, and cell tissue damage or death (Bates et al., 2019). This is linked to adverse health effects such as cardiovascular diseases, ischaemic heart disease, stroke, respiratory diseases and cancer.

ROS can enter the body through inhalation of PM with ROS bound to the surface, so-called particle-bound ROS. It can also be catalytically generated in vivo by inhaled PM stimulating biological redox reactions. This ROS pathway is referred to as oxidative potential (OP) (Bates et al., 2019; Chow et al.).

PM monitoring is relatively widespread today and exposure limits to PM exists such as through the EU directive on ambient air quality and cleaner air for Europe (Directive 2008/50/EC). Such monitoring, however, is indiscriminate between particle types and assumes that they all contribute equally to toxicity. Aerosol ROS concentration monitoring presents a potentially more accurate indicator of air

pollution related health risks instead of just scanning for PM, and a cheaper, faster and simpler solution compared to cellular or in vivo assays.

OP and particle-bound ROS levels can be estimated using various assays using chemical probes (Alessandro et al., 2023). In the case of OP it is common to use an assay that measures the depletion of chemical proxies for cellular reductants or oxidants, such as dithiothreitol (DTT), ascorbic acid (AA), or glutathione (GSH). In the case of particle-bound ROS it is instead common to measure the fluorescence of derivatives of chemical probes that readily react with PM, such as 9,10-bis (phenylethynyl) anthracene-nitroxide (BPEAnit) or 2,7-dichlorofluorescein diacetate (DCFH). Fluorescence is commonly measure in the arbitrary unit fluorescence intensity. BPEAnit reacts with PM to form the methylated derivative BPEAnit-Me, which is highly fluorescent, while DCFH forms the fluorescent derivative DCF. Aside from being sensitive to OP or particle-bound ROS, different probes are sensitive to different ranges of ROS in regards to chemical type.

1.1.1 Offline and online – traditional methods compared to real-time measurements (PINQ)

Traditional offline methods of ROS quantification are well established, having been used for decades in several studies all over the world (Venkatachari et al., 2005; Hung & Wang, 2001; Mudway et al., 2004). However, there are certain drawbacks to these methods that are worth evaluating. By nature, they present a delay between the sampling of air particles and the assessment of their ROS contents (Carlino et al., 2023). Typically, the air that is being analyzed must be passed through filters (Jovanovic et al., 2019), impingers (Montesinos et al., 2015), or impactors (Daher et al., 2011) to collect the particles, which can then be further processed for analysis. The delay between on-site aerosol collection and laboratory analysis is in general in the span of several days to weeks.

The main potential consequence of the delay, and to some extent the processing, is losses of volatile and short-lived species that lead to underestimation of particle-bound biochemically active ROS (Daher et al., 2011; Puthussery et al., 2020). While there are certain precautions that limit such losses, such as particle concentrators, the most effective way to eliminate them is to reduce time between collection and analysis.

To counter these drawbacks, several online real-time ROS-measurement devices have been constructed and tested. One such device of note is the Particle into Nitroxide Quencher (PINQ), which was first publicized in 2019 (Brown et al., 2019). This device continuously feeds sample air through an insoluble aerosol collector (IAC), in which the sampled air is cooled to allow for particle condensational growth. The particles are then mixed with a sample liquid containing the BPEAnit chemical probe in a vortex collector. The fluorescence of the resulting liquid is then continuously measured in a flow-through fluorimeter.

1.1.2 Sensitivity and limitations of different chemical probes

While there are many advantages of online ROS quantification apparatuses like the PINQ, the inherent sensitivity and limitations of different chemical probes need to be considered. BPEAnit, used in PINQ, is especially sensitive to methyl radicals generated by dimethyl sulfoxide (DMSO) in the probe reacting with particle-bound ROS, for example hydroxyl radicals (·OH) or organic peroxy radicals (ROO·) (Wang et al., 2025). However, there is a risk of underestimating ROS outside the range of sensitivity. BPEAnit is also stable over time, making it suitable for continuous online usage (Stevanovic et al., 2017).

In contrast, DCFH (one of the most popular probes for offline methods), is more nonspecific and reacts to a wide range of ROS (Venkatachari & Hopke, 2008), making it suitable for qualitative studies and a general approach. In addition, it is relatively inexpensive. However, the indiscriminate nature of DCFH leads to an inherent uncertainty regarding the ROS species present in the sample (Chen et al., 2010), also it is unstable and photo-labile.

In other words, applying multiple probes may ultimately be necessary to cover the full scope of ROS present in a single air sample. However, due to technical or resource limitations, this is not always possible. Understanding of the difference between probes and methods and their respective performance needs to be developed further. One study (Jovanovich et al., 2019) found a moderately strong correlation between the OP detected by BPEAnit and DCFH under the same conditions, but found a poor correlation to a third probe, DTT. As such, further study of the interchangeability of probes and methods is of interest.

1.1.3 Indoor air quality and ROS quantification as a field of research

Modern behavioral patterns mean that humans largely spend most of our time indoors, mainly at work, place of study, or at home (Schweizer et al., 2006; Matz et al., 2014). As such, understanding the impacts of exposure to indoor environments is an important puzzle piece to mapping trends in public health. While indoor air might seem benign, there are several common pathways of aerosol generation from indoor sources, including generation of ROS. Despite this, research data on PM from indoor sources is relatively scarce (Yao et al., 2023). Some research in the field has been done, but is somewhat limited in for example the choice of probe, particle source, and focus on OP rather than particle-bound ROS (Hu et al., 2023)

Cooking is commonly related to aerosol generation, although choice of fuel source and cooking method can drastically change the composition of particles. Cooking with electricity provided from a grid doesn't generate nearly as many aerosol particles in the household as burning of biomass such as wood (Li et al., 2021). Cooking with fats such as oil at high temperatures is a source of unsaturated fatty

acid aerosol particles, which can be oxidized to form peroxidic products, which is a type of ROS (Lu et al., 2023).

Generation of soot and carbonaceous nanoparticulate materials in indoor environments is commonly associated with biomass burning for cooking and temperature regulation but can also be generated through e.g. burning of candles and incense (Murr, 2008; Chuang et al., 2011). Soot is linked to the formation of ROS for example through formation of quinones and quinone-like structures on the particle surface, facilitated in part by characteristics such as the surface area of the particles as well as catalytic activity of the nanomaterial (Malmborg et al., 2025).

Secondary organic aerosols (SOA) are formed as volatile organic compounds (VOC) are oxidized, commonly by ozone, into less volatile compounds. These can in turn generate ROS (Tong et al., 2018). While VOCs are naturally generated by plants they can also be artificially introduced to the indoor environment, for example using oil and scent diffusers or air fresheners. Presence of oxidizing agents such as ozone in the indoor environment is usually dependent on concentrations in the outside air, but some indoor air purifiers use and release ozone.

ROS can also potentially be produced by processes involving human skin. Squalene is an oil that makes up 5-15 % of human sebum, keeping the skin moisturized and protected, and is easily transferred onto surfaces. The chemical makeup of squalene, containing six trans-oriented carbon–carbon double bonds, makes it particularly reactive. The addition of ozone across one of these double bonds forms a so-called Criegee intermediate. The Criegee intermediate can take several reaction pathways, and when reacting with water it produces hydrogen peroxide, which is a known ROS (Coffaro & Weisel, 2022).

1.1.4 Particle size and surface area contributions to ROS generation

Particle size and the correlation between decreasing particle size and increasing relative surface area are important toxicological characteristics (Nel, 2006; Oberdörster et al., 2005). In short, smaller particle sizes and larger surface areas are better at catalyzing ROS generation, leading to greater toxicity. Particles smaller than 100 nm diameter are particularly dangerous in this regard, but greater sizes still present a considerable risk.

1.1.5 Metals and catalytic ROS generation

Metals present pathways for ROS generation in PM. Metals that exist in more than one valence state, such as copper, iron, nickel, chromium, and lead can catalyze electron transfer that generates ROS, such as ·OH and hydrogen peroxide, and are found to positively correlate to oxidant production by PM in acellular systems (Ghio

et al., 2012; Pritchard et al., 1996). Therefore, characterization of metal contents in aerosols can help provide understanding of ROS concentration and toxicity.

1.1.6 Interaction between chemical probe and black carbon

Black carbon is a byproduct of incomplete combustion of hydrocarbons (Shu et al., 2023). When measuring ROS, scavenging at high concentrations of black carbon particles have been observed (Utinger et al., 2024). This is likely caused by surface chemistry of the black carbon particles, particularly the large surface area and hydrophobic nature of the surface. This allows black carbon particles to adsorb and inactivate the chemical probe, leading to underestimation of ROS concentration in the sample, or even a negative response. This needs to be taken into consideration when observing samples containing black carbon, such as soot.

1.2 Purpose

The purpose of this thesis is to assess the concentration of particle-bound ROS generated by some household sources of aerosols. This will be done with traditional offline methods, using DCFH as a chemical probe.

The sources of aerosols that will be analyzed are:

- Candles (C), smoke from burning household tapered candles
- Frying (F), frying of frozen pre-packaged hamburgers in rapeseed oil on an electric stove
- SOA (S), alpha-pinene oil and ozone (representing use of air fresheners or cleaning products)
- Incense (I), smoke from burning incense sticks
- Squalene (SqO), heated squalene oil and ozone (representing reaction between human skin and ozone)
- Combinations of the above primary sources, in the form of: Candles + ozone (CO), frying + ozone (FO), incense + ozone (IO), candles + SOA (CS), frying + SOA (FS), candles + frying (CF), candles + frying + SOA (CFS), as well as candles + frying + ozone (CFO)

The purpose is also to analyze data previously collected by the research group to further characterize the particles with respect to particle size, black carbon content, and metal content. This will be used to observe potential trends in how particle characteristics influence ROS concentration.

The ROS results will be compared with those of a novel online apparatus, PINQ, which was also previously collected by the research group. PINQ uses the BPEAnit probe.

1.3 Scope and limitations

The scope of this thesis includes extraction of particles from filters, from the sources described in section 1.2, and analysis of fluorescence when paired with a DCFH chemical probe. It also includes comparison of collected offline data with online data provided by the researchers from Aerosol Group at EAT (supervisors), as well as analysis of particle characteristics data also provided by the researchers.

It is possible to produce a calibration curve, for example from a series of standard H_2O_2 solutions, to be able to relate the results from spectrofluorometer analysis (fluorescence intensity/µg) to H_2O_2 equivalents (Jovanovic et al., 2019). Due to time constraints this step was skipped.

Previous work by the research group has included the construction of PINQ, real-time measurements with PINQ, and collection of particles onto filters during experiments conducted in the aerosol chamber as well as real time measurements of particle characteristics (particle size and black carbon contents) and offline metal analysis.

2 Method

2.1 Generation of particles

Prior to the start of this thesis, particles were generated in a room-sized climate controlled experiment chamber, an aerosol chamber, in a series of experiments with different set-ups. Each experiment was repeated 2-5 times, for a duration of two hours each.

- Candles (C): A household tapered candle was lit and let burn for 20 minutes. A rotating fan was placed in the aerosol chamber to blow on the candle flame, making it flicker, to propagate generation of soot.
- Frying (F): 10 ml of rapeseed oil was added to a non-stick pan and heated. Once the oil reached 100 °C, a pre-made frozen hamburger patty was added to the pan. It was flipped every five minutes for a total cooking time of 15 minutes. The temperature of the pan was monitored to not exceed 200 °C. After 20 minutes a second burger was cooked following the same method, and 20 minutes following that a third burger was cooked.
- SOA (S): Air with a flow rate of about 1 L/min was blown over a container of alpha-pinene oil to promote vaporization. Simultaneously, an ozone generator generated ozone to a concentration of about 30 ppm in the aerosol chamber. The reaction between the alpha-pinene and the ozone is the source of the SOA.
- Incense (I): Four incense sticks were lit and let burn until they burned out. This took barely one hour.
- Squalene (SqO): A container of squalene oil was heated to 200 °C and air was blown above the container at a flow rate of 3.6 L/min. Squalene was vaporized until the concentration of it in the chamber air reached 300 µg/m3. At this point, the ozone generator was turned on, which marked the start of the experiment time.

When combining experiment types, they were conducted the same way as described above, only simultaneously. During each experiment, the air in the aerosol chamber was drawn through two separate Dekati Gravimetric Impactors at a flow rate of about 70 L/min, allowing for collection of particles of size PM 2.5 onto two separate 70 mm filters. Between each experiment all air was emptied out of the chamber, and the chamber was cleaned.

How many times the experiments were repeated for each particle type, and how many of these were used in analysis, is presented in table 1.

Table 1: Number of experiments per particle type

Particle type	C	F	S	I	CO	FO	IO	SqO	CS	FS	CF	CFS	CFO
Number of experiments performed	5	4	3	4	2	2	2	2	4	4	3	3	2
Number of experiments used in analysis	4	3	3	3	2	2	2	2	3	3	3	3	2

2.2 Determination of mass of particles collected on filters

The filters with particles were stored in a freezer in the aerosol lab. Before extractions, the filters were brought to AMM (Arbets- och miljömedicin) lab and stored in a climate-controlled chamber for 24 hours. This was to stabilize filter mass to adjust to ambient conditions such as relative humidity and temperature, before being weighed also at the AMM lab. Prior to the experiments the filters were weighed in the same way, and the post-experiment weighing was to determine particle mass on the filters. After weighing they were brought back in storage in the freezer.

2.3 Extractions of particles from filters

To analyze the aerosol particles, they need to be extracted from the filters they were collected onto. They can then be put into well plates and mixed with the chemical probe for analysis.

2.3.1 Preparing the vials and determining vial mass

Before extractions the inside of glass flat-bottom vials were washed twice with deionized water and once with methanol, then completely dried inside a fume hood. The vials were then capped and labeled with stickers. The empty vials with caps and stickers were weighed three times in succession. The average mass of the three measurements was used to determine vial weight.

Empty vials were also used as reference to account for subtle changes in vial mass due to ambient conditions, rather than particle mass after extraction phase. Initially, weighing of a control vial for reference was limited to about once per day. However, partway through the process, it was discovered that the empty vials exhibited large natural variation in mass which required more careful methods. At this point, two reference vials of the same type were always weighed together with each set of empty vials. The sets all consisted of six empty vials with only a few exceptions, making a total of eight vials weighed in succession including references. The reason for this is that on average, six vials were used to contain the particles from one extraction, making groups of six vials a "set".

2.3.2 Extraction

The filters were put into individual laboratory bottles with a diameter slightly greater than that of the filters. Methanol, about 25 ml, was added to the bottles to submerge the filters. The bottles were then sonicated for 15 minutes to extract the particles from the filters into the methanol suspension. The particle suspension was poured into round bottom flasks. Because each experiment using the PINQ generated two filters of collected particles, the methanol suspension from corresponding filters were poured into the same round bottom flasks. After initial sonication the filters were flipped upside down, and the same process was repeated for a second and third sonication. The temperature of the water bath in the sonicator was measured between each sonication to ensure the temperature did not exceed 35 °C. During trial runs, it was found that when measuring the temperature during sonication, it did not exceed the temperature measured after sonication was done. It was therefore assumed that simply measuring temperature between and after sonication was enough to ensure that it did not reach undesirable levels at any point during the process.

Once particles had been extracted from the filters, the filters were allowed to airdry inside the fume hood until the end of the day. They were then put into a desiccator overnight and weighed the next or the following few days. After weighing, the filters were discarded.

The round bottom flask was put into a rotary evaporator and submerged in a water bath maintaining 30 °C. A pump generated a pressure of 150 mbar in the flask and most of the methanol was evaporated from the suspension. The volume of suspension left in the round bottom flask was not measured exactly, but it was reduced to around 8-12 ml. The time spent in this phase varied depending on how much liquid was in the suspension to begin with.

The remaining suspension was pipetted and distributed between four to six flat bottom vials. The vials were then put into a heating block which warmed the vials to 34 °C and affixed under a set of nozzles. Nitrogen gas was blown onto the surface of the suspension through the nozzles to further evaporate the methanol. The flow

of nitrogen was adjusted to create only slight rippling on the surface of the suspension, to prevent splashing and losses of particles.

Once all the methanol had been evaporated the vials were kept capped inside a laminar flow cabinet and cooled to room temperature before weighing. In cases where weighing the vials could not be performed the same day as the extraction of particles, they were kept refrigerated.

2.3.3 Determination of mass of extracted particles

The temperature stabilized vials with particles were weighed along with empty vials that served as reference. The weighing was repeated three times, and the average of the three measurements was used to determine vial and particle mass. The difference in reference vial mass before and after extraction and evaporation was subtracted from the vials containing the particles to obtain particle mass. Average of two reference vials were used for majority of measurements, on few occasions (due to technical issues and use of different sizes of vials) when reference was missing, an average of reference vials from day before and after was used as proxy to calculate the mass of the particles.

As the decision to use proxy references was made after analysis had been performed, this affects the dilution scheme as described in section 2.4.2.3 for affected vials and plates. The final concentrations do not differ greatly compared to the baseline, and the regression lines as described in section 2.4.3 have been adjusted accordingly, to ensure accurate results.

The filters themselves were also weighed after being dried in the desiccator and the difference in mass was used to determine the rate of extraction from the filters, as well as a point of reference to see if the mass of particles determined by weighing the vials appeared accurate.

2.4 ROS analysis

2.4.1 PINQ

The ROS-concentration during experiments was determined in real-time using the PINQ instrument and determined in units of fluorescence intensity/µg.

The PINQ operates as follows: The air flow in the PINQ is 16.7 L/min, or 1 m^3/h. Particles in the sampled air are mixed with steam, and as it cools, the steam condenses on the particles. This causes the particles to increase in size, so-called condensational growth. The mixture of air, particles and steam is sent into a wetted-wall cyclone, also referred to as a vortex collector. Just before the cyclone, at the

point labeled sample liquid in, a 4 µM solution of BPEAnit in DMSO (flow rate 1 ml/min) is added. The chemical pathway of BPEAnit to the fluorescent derivative BPEAnit-Me is illustrated in figure 1.

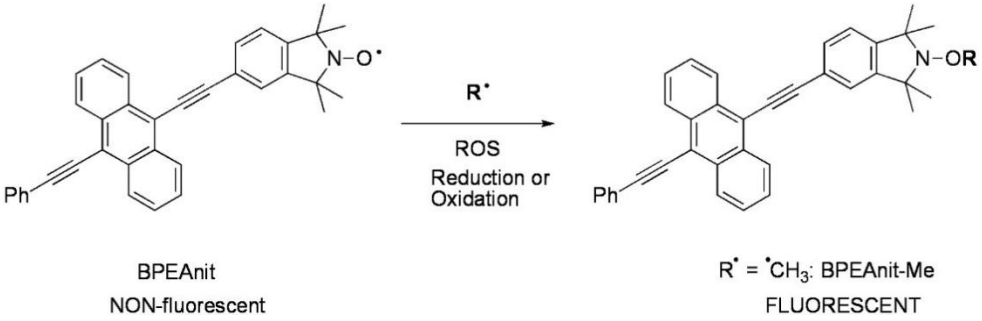

Figure 1: BPEAnit probe to BPEAnit-Me fluorescent derivative pathway (Miljevic et al., 2010)

The particles in the air stream stick to the edges of the cyclone, and the liquid is extracted continuously from the bottom at a rate of 1 ml/min. This liquid then passes a measuring cell and is irradiated by a laser of wavelength 450 nm. An Ocean HDX spectrophotometer measures fluorescens at 480-486 nm. Half of the time, changed every five minutes, the air is cycled through a HEPA filter to read the contribution to fluorescence from the gas-phase without any particles. By removing this baseline from the results, it is possible to deduce the ROS-contribution from only the particle-bound ROS. A schematic of the PINQ is illustrated in figure 2.

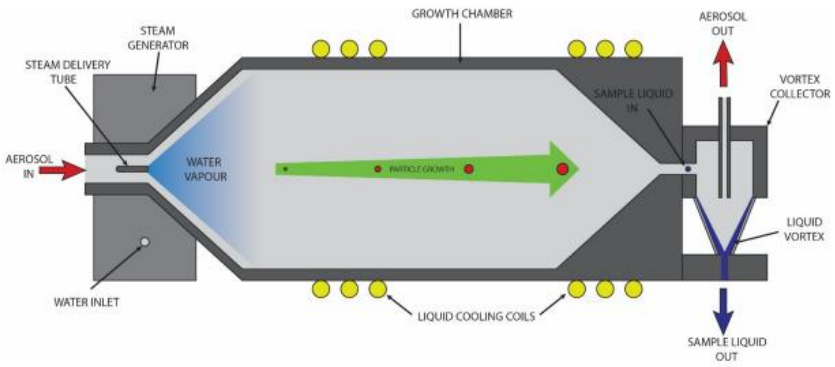

Figure 2: Schematic of the PINQ (Bron et al., 2019)

2.4.2 Traditional method

2.4.2.1 Preparation of chemical probe DCFH

To prepare the chemical probe, 0.0049 g of DCFH was dissolved in 10 ml of methanol and distributed in 500 µl black Eppendorf tubes, then stored in a freezer

in the aerosol lab. It was important to reduce exposure to light as the DCFH probe is photosensitive.

Before using the probe, an Eppendorf tube was removed from the freezer and thawed. The contents were poured into a 15 ml black tube, and 2 ml of 0.01 nmol NaOH was added. This stood at room temperature for 30 minutes before 10 ml of Hank's balanced salt solution (HBSS) was added. HBSS is commonly used in the DCFH assay as a reaction buffer (Kim & Xue, 2020). At this point the probe was ready for use.

2.4.2.2 Preparation of particle stock solution

Several experiments were conducted on each particle type, as described in section 2.1. Each experiment produced four to six vials of extracted particles. At least two of the different experiments per particle type were selected for ROS analysis. From each selected experiment, only one of the vials produced was used for analysis. In cases where three or more experiments per particle type had been performed, three vials (one per experiment) were selected. From the candle experiments, four vials were selected, with two of them coming from the same experiment. In the case of SOA, experiments one and two were accidentally mixed during the extraction process. Two vials from this mixed batch were selected.

To the vials, ultrapure water was added to achieve a stock solution with particle concentration of 1350 µg/ml. In the cases where the particle mass in the vial was too low to achieve this, the particles were instead diluted to a concentration of 500 µg/ml and in some rare cases even lower. The vials were then sonicated for at least 30 minutes, during which it was ensured that the water bath did not exceed 35 °C, to disperse the particles in the suspension.

After sonication, the stock solution was pipetted into 2 ml clear Eppendorf tubes and diluted with HBSS to a particle concentration of 135 µg/ml and a volume of 2 ml. These made up the starting point for the dilution scheme described below, and visualized in figure 3.

2.4.2.3 Dilution scheme, preparation and reading of well-plates

This describes the dilution scheme baseline, as it was conducted for all vials and well plates. Since a change in assumption of particle mass in a few of the vials, as described in section 2.3.2, was made after all dilution schemes, the final concentration in the wells varies slightly.

Seven additional Eppendorf tubes were used to create the dilution scheme for each stock solution. To one of them, 0.5 ml of HBSS was added, while 1 ml of HBSS was added to the rest. 1 ml of the solution from tube one was pipetted into the tube containing 0.5 ml of HBSS, and 1 ml of this solution was then pipetted into a tube containing 1 ml of HBSS and so on. Before diluting from one tube to the next, the tube that had its contents pipetted was mixed using a vortex mixer to ensure even

distribution of particles throughout the suspension. The dilution scheme is illustrated in figure 3.

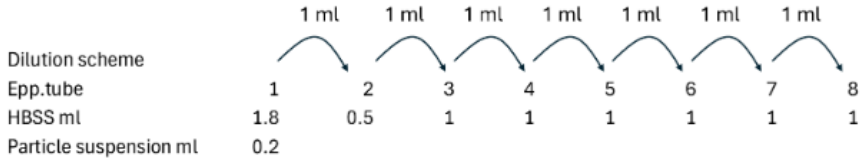

Figure 3: Particle dilution scheme

Note that while in figure 3 it says that tube 1 contains 1.8 ml HBSS and 0.2 ml particle suspension, this is only true for the vials that were diluted to a concentration of 1350 µg/ml. This was adjusted for the other vials so that the particle concentration in tube 1 always ended up as 135 µg/ml. The particle concentrations and volumes of Eppendorf tubes after dilution are illustrated in table 2.

Table 2: Final particle concentrations and volume in dilution scheme

Epp. Tube	E1	E2	E3	E4	E5	E6	E7	E8
Particle concentration (µg/ml)	135	90	45	22.5	11.25	5.6	2.8	1.4
Final volume (ml)	1	0.5	1	1	1	1	1	2

The 96-well plates used in the spectrofluorometer were first prepared by adding 50 ml of HBSS to wells 2B-C as well as 11,12B-G. Then 150 µl of the 135 µg/ml solution from tube 1 was added to wells 2B-C and 3B-E. Then 150 µl was added to wells 3B-D from tube 2. Wells B-G of columns 5-10 were filled with 150 µl of the remaining tubes in order of descending concentration. Finally, 50 µl of the prepared DCFH-probe was added to wells B-G of columns 3-12. Columns 11-12 were used as reference wells, representing background noise from HBSS and the probe. The average of the fluorescence intensity from these wells were subtracted from the average of the fluorescence intensity of the wells from columns 3-9, giving the final average fluorescence intensity per particle concentration (fluorescence intensity/µg/ml). The two wells in column 2 were used to check that the fluorescence intensity of a particle suspension without any probe did not stray too far from 0, as would be expected.

A schematic of the well plates and final particle concentrations in each well is illustrated in figure 4.

	1	2	3	4	5	6	7	8	9	10	11	12
A												
B		150 µl E1, 50 µl HBSS, 101 µg/ml	150 µl E1, 50 µl DCFH, 101 µg/ml	150 µl E2, 50 µl DCFH, 68 µg/ml	150 µl E3, 50 µl DCFH, 34 µg/ml	150 µl E4, 50 µl DCFH, 17 µg/ml	150 µl E5, 50 µl DCFH, 8 µg/ml	150 µl E6, 50 µl DCFH, 4 µg/ml	150 µl E7, 50 µl DCFH, 2 µg/ml	150 µl E8, 50 µl DCFH, 1 µg/ml	150 µl HBSS, 50 µl DCFH	150 µl HBSS, 50 µl DCFH
C		150 µl E1, 50 µl HBSS, 101 µg/ml	150 µl E1, 50 µl DCFH, 101 µg/ml	150 µl E2, 50 µl DCFH, 68 µg/ml	150 µl E3, 50 µl DCFH, 34 µg/ml	150 µl E4, 50 µl DCFH, 17 µg/ml	150 µl E5, 50 µl DCFH, 8 µg/ml	150 µl E6, 50 µl DCFH, 4 µg/ml	150 µl E7, 50 µl DCFH, 2 µg/ml	150 µl E8, 50 µl DCFH, 1 µg/ml	150 µl HBSS, 50 µl DCFH	150 µl HBSS, 50 µl DCFH
D			150 µl E1, 50 µl DCFH, 101 µg/ml	150 µl E2, 50 µl DCFH, 68 µg/ml	150 µl E3, 50 µl DCFH, 34 µg/ml	150 µl E4, 50 µl DCFH, 17 µg/ml	150 µl E5, 50 µl DCFH, 8 µg/ml	150 µl E6, 50 µl DCFH, 4 µg/ml	150 µl E7, 50 µl DCFH, 2 µg/ml	150 µl E8, 50 µl DCFH, 1 µg/ml	150 µl HBSS, 50 µl DCFH	150 µl HBSS, 50 µl DCFH
E			150 µl E1, 50 µl DCFH, 101 µg/ml		150 µl E3, 50 µl DCFH, 34 µg/ml	150 µl E4, 50 µl DCFH, 17 µg/ml	150 µl E5, 50 µl DCFH, 8 µg/ml	150 µl E6, 50 µl DCFH, 4 µg/ml	150 µl E7, 50 µl DCFH, 2 µg/ml	150 µl E8, 50 µl DCFH, 1 µg/ml	150 µl HBSS, 50 µl DCFH	150 µl HBSS, 50 µl DCFH
F					150 µl E3, 50 µl DCFH, 34 µg/ml	150 µl E4, 50 µl DCFH, 17 µg/ml	150 µl E5, 50 µl DCFH, 8 µg/ml	150 µl E6, 50 µl DCFH, 4 µg/ml	150 µl E7, 50 µl DCFH, 2 µg/ml	150 µl E8, 50 µl DCFH, 1 µg/ml	150 µl HBSS, 50 µl DCFH	150 µl HBSS, 50 µl DCFH
G					150 µl E3, 50 µl DCFH, 34 µg/ml	150 µl E4, 50 µl DCFH, 17 µg/ml	150 µl E5, 50 µl DCFH, 8 µg/ml	150 µl E6, 50 µl DCFH, 4 µg/ml	150 µl E7, 50 µl DCFH, 2 µg/ml	150 µl E8, 50 µl DCFH, 1 µg/ml	150 µl HBSS, 50 µl DCFH	150 µl HBSS, 50 µl DCFH

Figure 4: Distribution and particle concentration of well plates

After pipetting into the wells was finished, a lid was put on the plates, and they were allowed to incubate at 37 °C for 3 hours. This was to allow ample time for particles to react with the probe, under conditions as close to the human body as possible. The chemical pathway (exemplified) from DCFH to the fluorescent derivative DCF is illustrated in figure

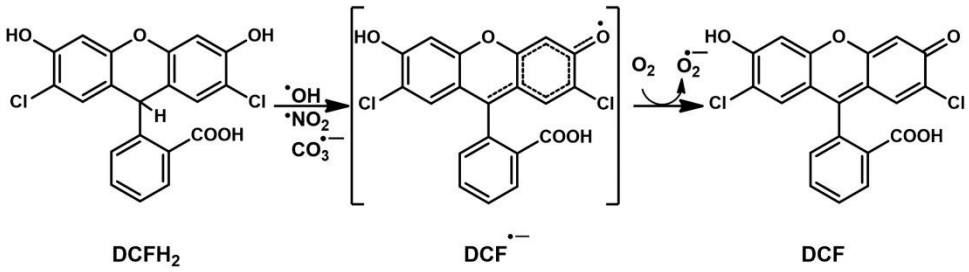

Figure 5: DCFH probe to DCF fluorescent derivative pathway (Prolo et al., 2018)

When 3 hours had passed, the plates were read in the spectrofluorometer, giving ROS-concentration approximated in units of fluorescence intensity/µg/ml at excitation wavelength 485 nm and emission wavelength 530 nm. This was then divided by the volume of suspension and probe in the wells, making the unit fluorescence intensity/µg

2.4.3 Statistical analysis

The average fluorescence intensity of each concentration was plotted and fitted with a linear regression which intersected at 0. The amount of data points included in the linear regression was adjusted until a R^2 value of generally 0.97 or higher was achieved, which indicates a linear response. The reason for this was to avoid the effects of scavenging and noise, which are more prominent at higher particle concentrations. This generally, and at the very least, meant only using data up to the fourth lowest concentration but varied from experiment to experiment.

The slope of the linear regression from each plate gave the ROS concentration, represented as a function of fluorescence intensity per µg of particles. By plotting the average of readings of the same particle type in a bar chart, it was possible to compare ROS concentration of the different particle sources. By plotting all the slopes from the plate readings, grouped by experiment type, it was possible to analyze variations between experiments.

Standard deviation was calculated using the standard deviation formula, stdev = $\sqrt{\frac{\sum(x-\bar{x})^2}{n}}$, where x is an individual data value, $\bar{x}$ is the population mean, and n is the number of values in the population. If the lower limit of the deviation reached into the negatives, it was cut off at 0.

2.4.4 Blanks

A set of filters having collected particles from “clean” ambient air also underwent the same process of extraction and analysis. These produced three “blanks” which could be used for corrections or baseline comparisons. All three blanks produced results close to 0 fluorescence intensity/µg, and as such weren’t used for further consideration.

2.5 Particle characterization

A scanning mobility particle sizer, SMPS (TSI) was used to measure size distribution and calculate average particle size. The aerosol sampling flow of the SMPS was 0.3 L/min, and the sheath flow 3 L/min. Particle detection range was 14 to 673 nm.

An aethalometer was used to determine the concentration of black carbon among the particles. The sampling flow in the aethalometer was 2 L/min, and it generated one point of data every minute.

Aside from the filters collecting particles for extraction, smaller filters were placed in a DustTrak with a sampling flow of 2 L/min. After sampling they were kept frozen and then sent to AMM to be weighed. The filters were then halved, and analysis of metal contents was conducted using inductively coupled plasma mass spectrometry.

3 Results

3.1.1 Offline measurements with DCFH assay – "Traditional method"

Average ROS concentration, represented by average fluorescence intensity/µg, per particle type as detected by the spectrofluorometer using the traditional method is presented in figure 6.

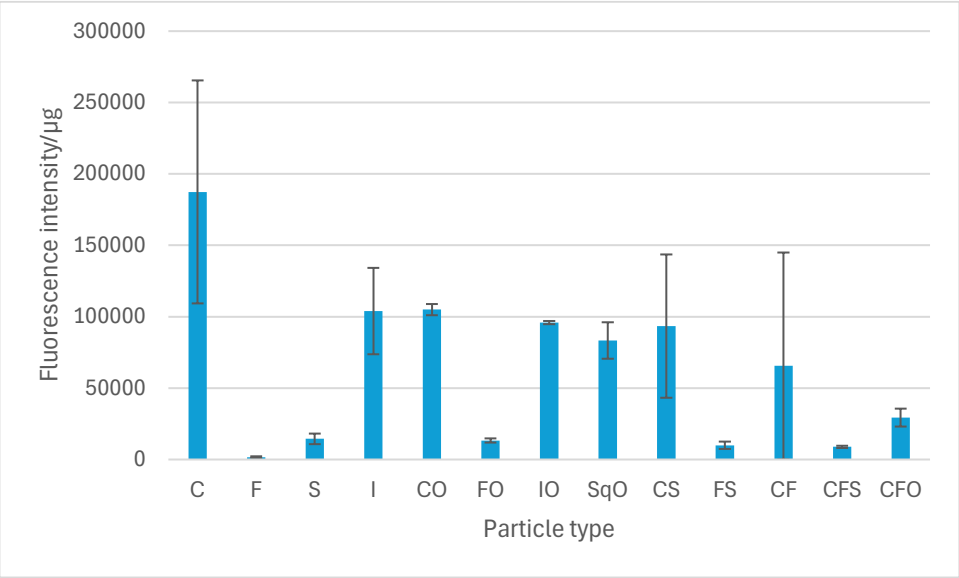

Figure 6: Average fluorescence intensity per particle concentration by particle type, traditional method

ROS has been detected in all the observed samples. The greatest average ROS concentration was detected in the candle samples, at around 190 000 FI/µg. It is followed by candles + ozone and then incense, both around 100 000 FI/µg. Incense + ozone, candles + SOA (with ozone), squalene (with ozone), and candles + frying all have an average between 80-95 000 FI/µg. Frying, SOA, frying + ozone, frying + SOA, and candles + frying + SOA all have an average of around or below 10 000 FI/µg.

However, as indicated by the standard deviations, there are uncertainties to comparing ROS concentrations by particle type. This is illustrated by comparing results from individual vials in figure 7. The number at the end denotes which experiment the vial was taken from.

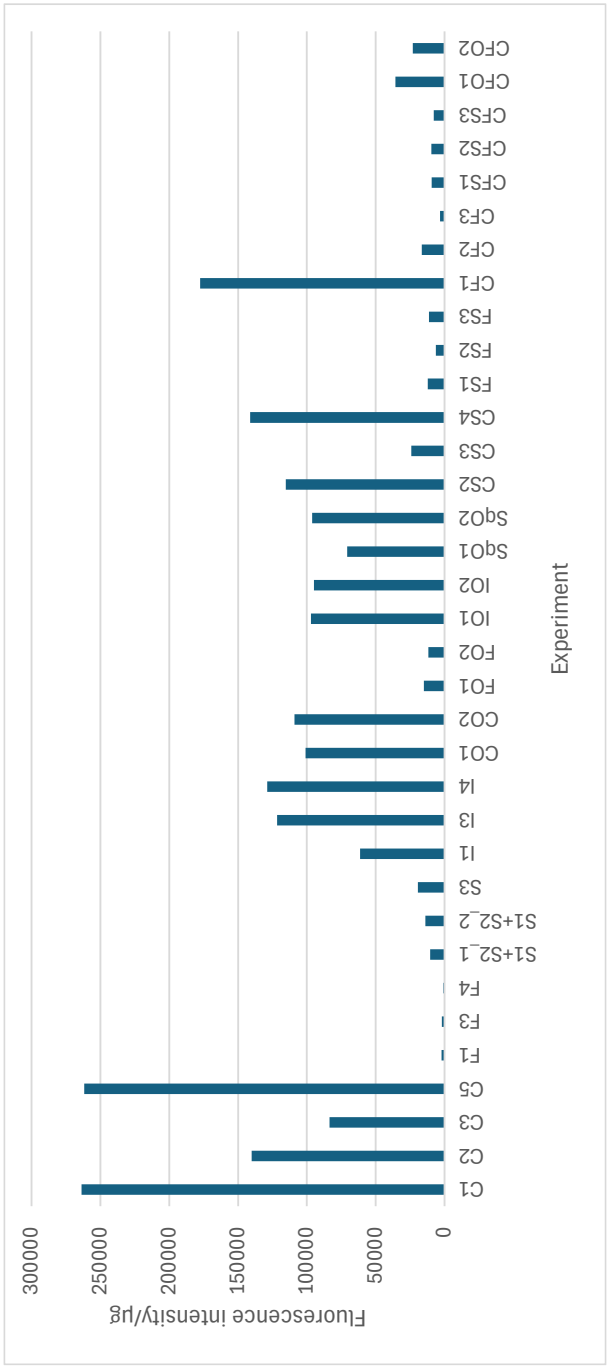

Figure 7: Fluorescence intensity/µg per each vial analyzed

As evidenced by figure 6, certain vials give rise to great variations of fluorescence intensity within the same particle type. While candle experiments 1 and 5 show fluorescence intensity of similar magnitude, they are almost three times greater than the counts from the vials from experiment 3. Candles + frying 1 is at least 56 times greater than candles + frying 3. Candles + SOA 4 is five times greater than candles + SOA 3, and incense 4 is two times greater than incense 1.

3.2 Particle characterization

3.2.1 Particle size

Average particle size in nm of each particle type is presented in figure 8. The SMPS analyzed particles from every experiment, as described in table 1, performed by the research group. The data was then summarized as average particle size per experiment occasion, so for example average particle size for candle experiments 1-5. This then became the basis for average particle size per particle type, as presented in figure 8.

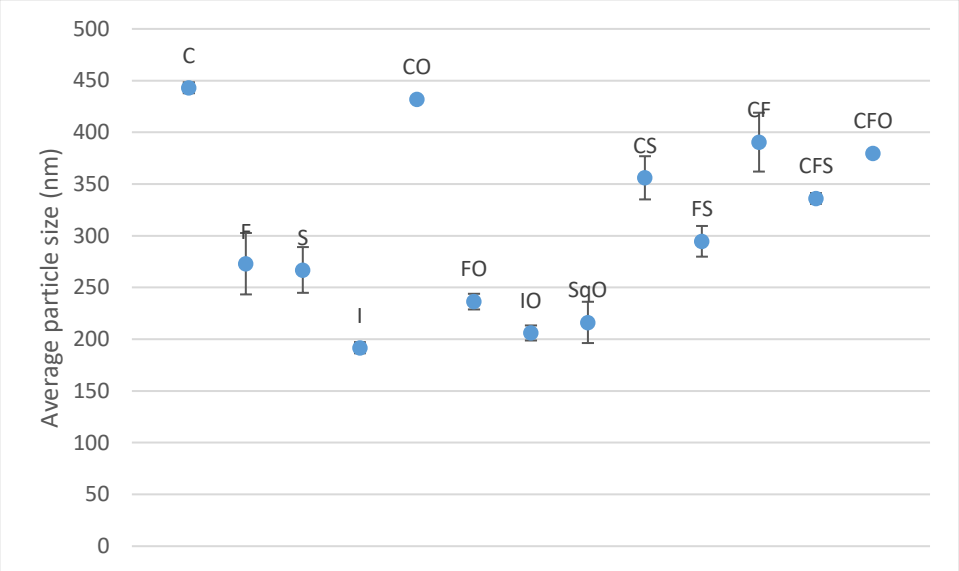

Figure 8: Average size of each particle type

The particles emitted from candles (in any combination) are of greater size than the rest of the particle types, with the greatest average particle size coming from just candles at 443 nm. The smallest particle sizes come from experiments involving incense, at around 200 nm.

3.2.2 Black carbon concentration

Black carbon concentration in ng/m^3 per particle type is presented in figure 9.

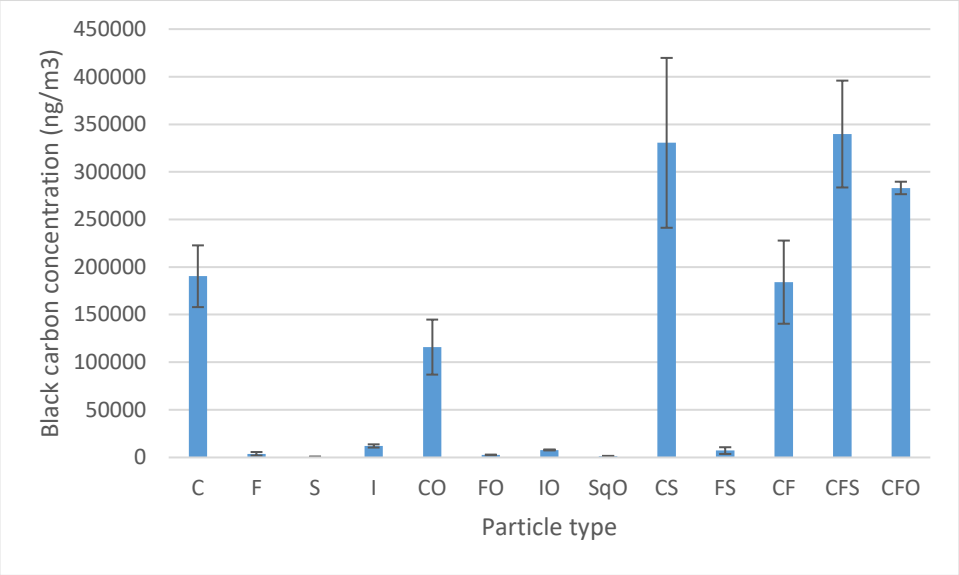

Figure 9: Black carbon concentration in ng/m3 per particle type

Black carbon is mainly, almost solely, present in experiments where candles are involved. Some, but to a lesser extent, can also be detected from experiments involving incense.

3.2.3 Metal content

Average concentration of metals per particle type by mass is presented in figure 10. Not all particle types or combinations were analyzed for metal contents, hence the limited categories. The reason for this is that it was assumed that for particle combinations where ozone was added, no significant change in metal concentration would be observed.

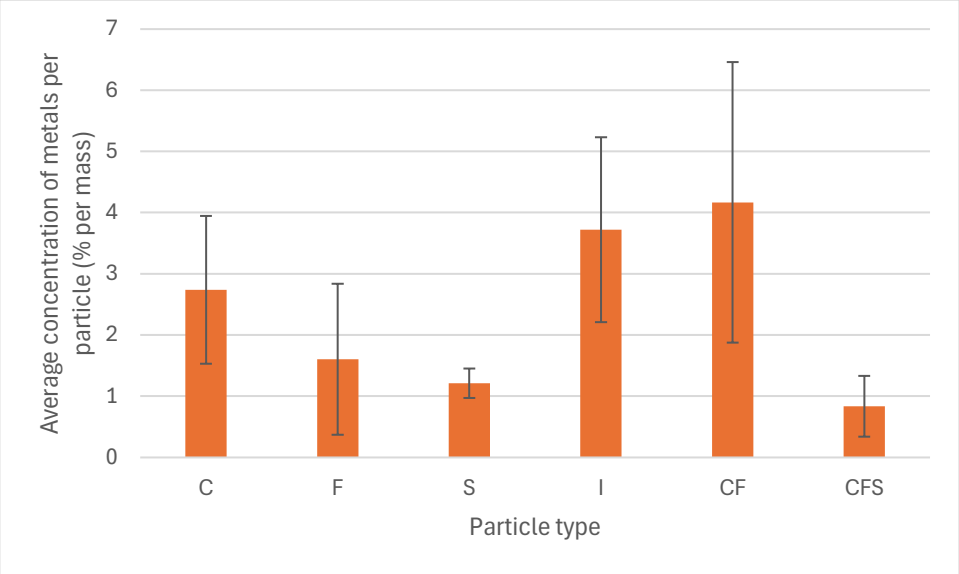

Figure 10: Average concentration (%) of metals per particle mass

The greatest average concentration of metals is present in the sampled candles+frying filters, at around 4 % by mass, followed by incense. Candles+frying+SOA has the lowest concentration of metals, less than 1 %. The measured metal concentration of CF and CFS, despite being combinations of individual particle types, is not the mean of the individual particle types.

Average concentration by mass of five key metals are presented in figures 11-15. These metals are copper, iron, nickel, lead, and chromium.

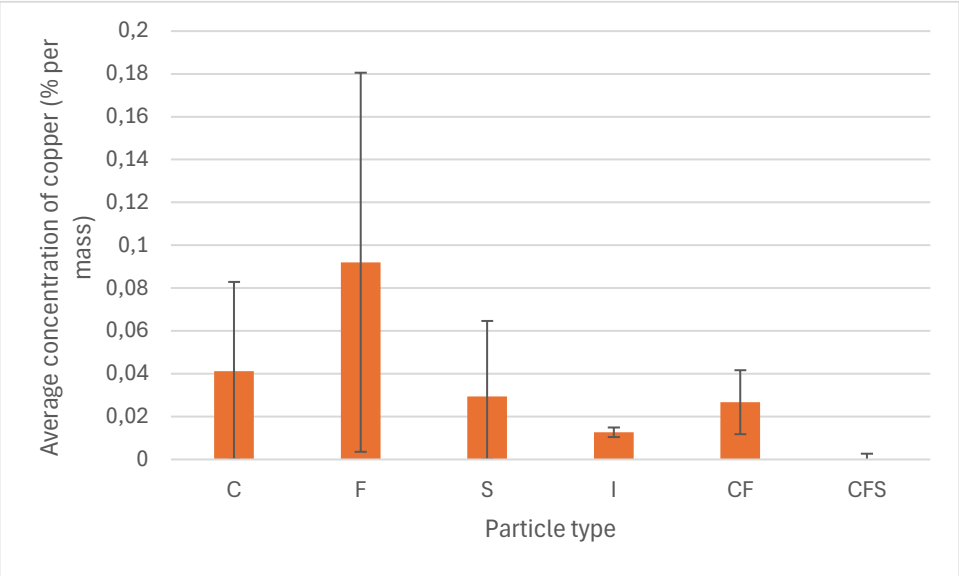

Figure 11: Average concentration (%) of copper per particle mass

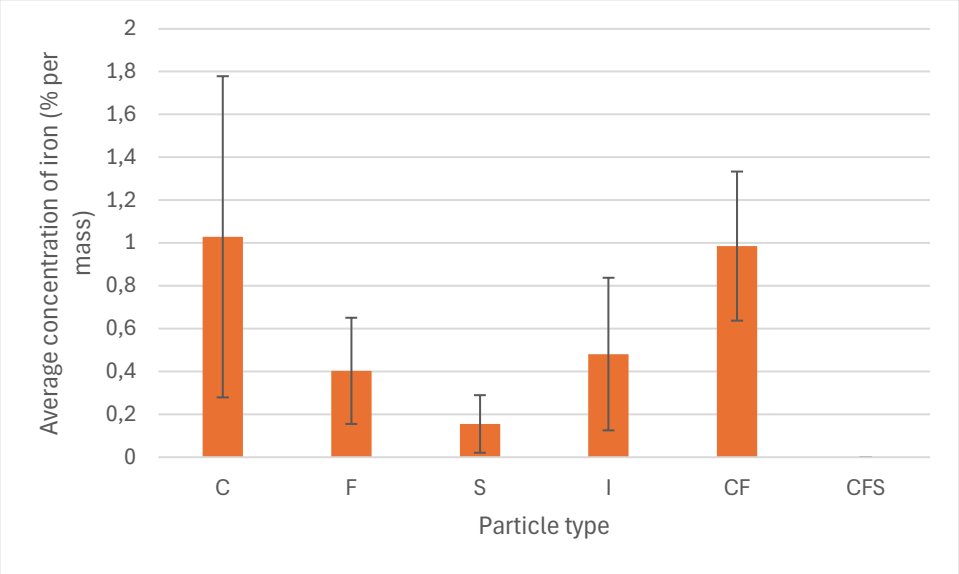

Figure 12: Average concentration (%) of iron per particle mass

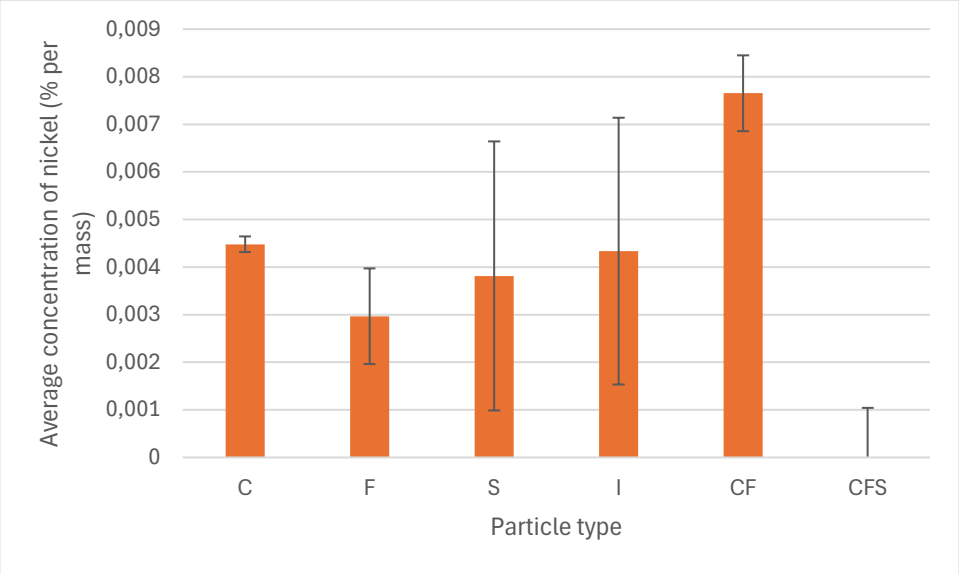

Figure 13: Average concentration (%) of nickel per particle mass

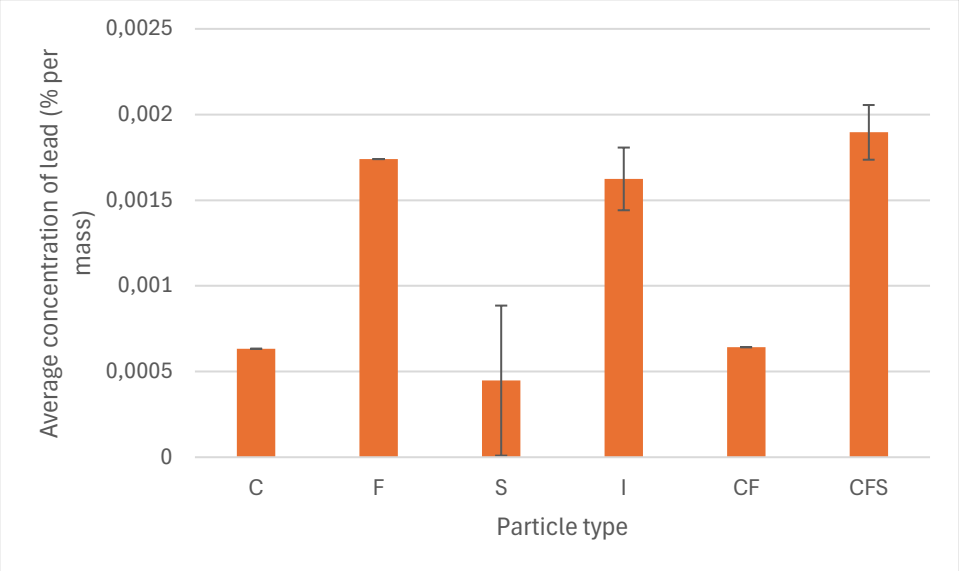

Figure 14: Average concentration (%) of lead per particle mass

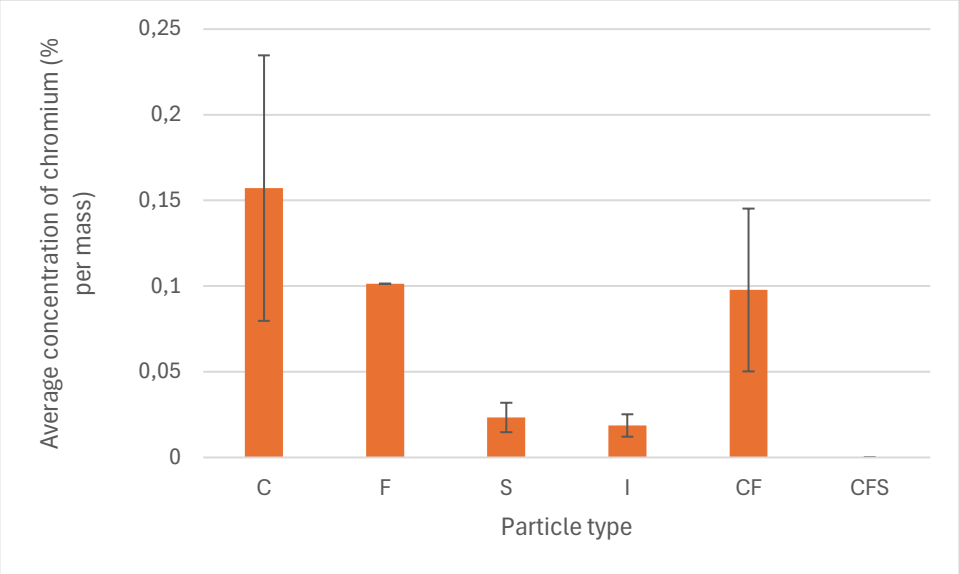

Figure 15: Average concentration (%) of chromium per particle mass

All measured particle types show some concentration of key metals. Candles + frying + SOA stands out as having concentrations below or close to the limit of detection for all key metals yet having the highest concentration of lead. The metal present in the highest concentration in all sampled particles except Candles + frying + SOA is iron.

Other metals that make up a greater portion of mass concentration, such as potassium and phosphorus, are not analyzed further because they do not have the characteristics necessary to propagate ROS generation.

Spearman correlation coefficient between ROS concentration for sampled particle types (C, F, S, I, CF and CFS) and metal concentration by particle type is presented in table 3.

Table 3: Spearman correlation coefficient between ROS concentration and metal concentration by particle type

	Spearman correlation coefficient ROS:Metal
Total metal concentration	0.60
Chromium	0,257
Iron	0,771
Nickel	0,771
Copper	-0,0857
Lead	-0,543

A moderate to strong positive correlation between ROS concentration and metal concentration is implied for total metal concentration, iron, and nickel. A weak positive correlation is implied for chromium. A weak to moderate negative correlation is implied for copper and lead.

3.3 PINQ

The results of the online ROS measurements using the PINQ are presented in figure 16.

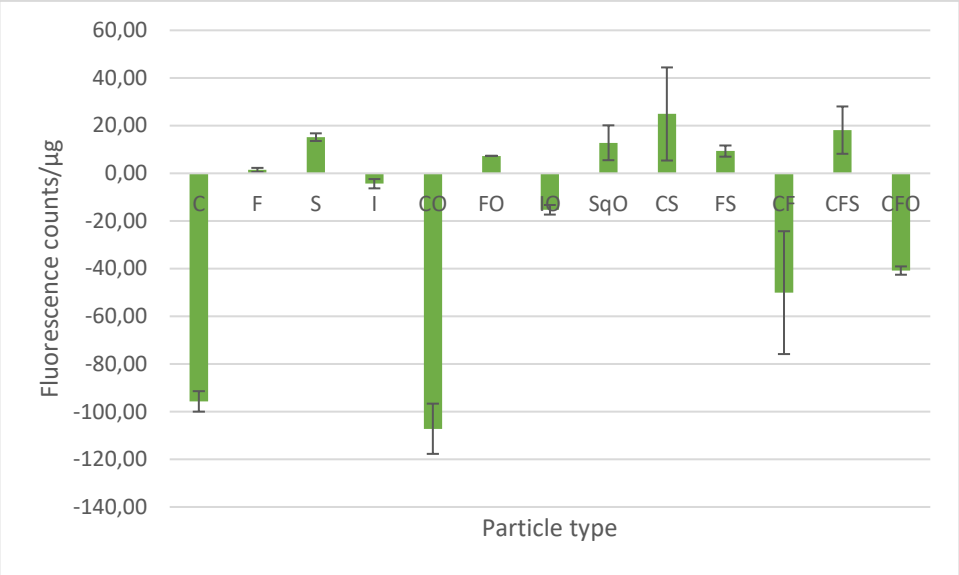

Figure 16: PINQ ROS online measurement results

Several particle types, particularly most of the candle combinations and those that include incense, display negative fluorescence (negative concentrations of ROS). Of the ones that exhibit positive concentrations they are of similar magnitude except frying which is close to 0.

3.4 Comparison

A comparison between the ROS concentration assessed with the traditional method and PINQ respectively is shown in figure 17.

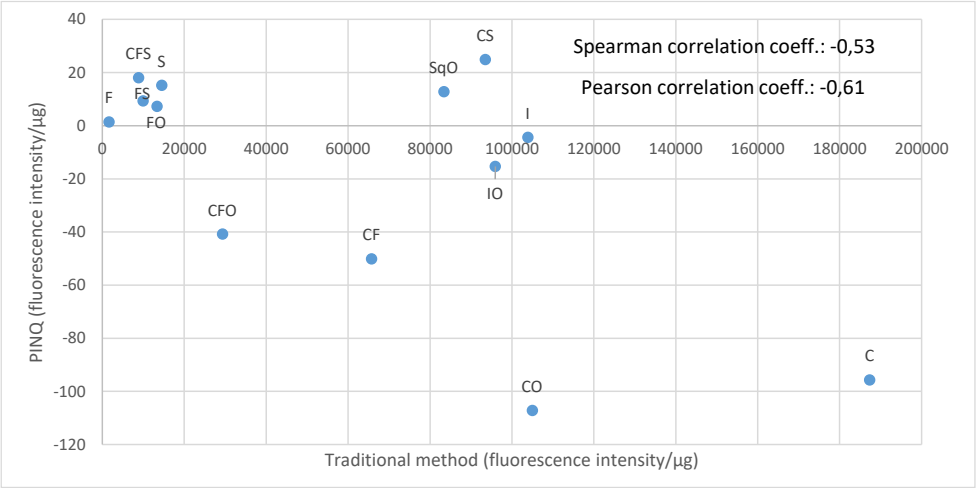

Figure 17: Comparison between ROS fluorescence intensity results for traditional method and PINQ, with correlation coefficients

The Spearman correlation coefficient of -0.53 and the Pearson correlation coefficient of -0.61 suggests a somewhat negative correlation between the samples, i.e. response from the PINQ decreases as response from the traditional method increases.

4 Discussion

4.1 Key findings from offline method and possible correlations to particle characteristics

Using the traditional offline method, ROS was detected in all the sampled particles. The data suggests that candles produced the most ROS, followed relatively closely by incense and squalene. Frying and SOA show the least presence of ROS. Whether the difference in average ROS concentration between two particle types is statistically significant or not is determined by two-tailed heteroscedastic t-testing, and is presented in figure 18. P-values lower than 0.05, suggesting the difference in response between particle types is statistically significant, are highlighted in green. P-values greater than 0.05, suggesting statistically insignificant difference in response, are highlighted in dark teal.

t-test	C	F	S	I	CO	FO	IO	SqO	CS	FS	CF	CFS	CFO
C		0,03	0,03	0,17	0,16	0,03	0,14	0,10	0,16	0,03	0,16	0,03	0,04
F	0,03		0,04	0,04	0,02	0,07	0,00	0,10	0,12	0,04	0,37	0,00	0,14
S	0,03	0,04		0,05	0,00	0,72	0,00	0,11	0,16	0,23	0,46	0,15	0,22
I	0,17	0,04	0,05		0,97	0,05	0,75	0,47	0,82	0,05	0,58	0,05	0,06
CO	0,16	0,02	0,00	0,97		0,01	0,25	0,32	0,78	0,01	0,56	0,02	0,02
FO	0,03	0,07	0,72	0,05	0,01		0,00	0,11	0,15	0,25	0,45	0,18	0,22
IO	0,14	0,00	0,00	0,75	0,25	0,00		0,50	0,95	0,00	0,64	0,00	0,05
SqO	0,10	0,10	0,11	0,47	0,32	0,11	0,50		0,81	0,10	0,79	0,11	0,10
CS	0,16	0,12	0,16	0,82	0,78	0,15	0,95	0,81		0,14	0,70	0,14	0,21
FS	0,03	0,04	0,23	0,05	0,01	0,25	0,00	0,10	0,14		0,42	0,63	0,18
CF	0,16	0,37	0,46	0,58	0,56	0,45	0,64	0,79	0,70	0,42		0,42	0,58
CFS	0,03	0,00	0,15	0,05	0,02	0,18	0,00	0,11	0,14	0,63	0,42		0,19
CFO	0,04	0,14	0,22	0,06	0,02	0,22	0,05	0,10	0,21	0,18	0,58	0,19	

Figure 18: Two-tailed heteroscedastic t-testing of average ROS-concentration by particle type, represented by fluorescence intensity, for the offline method

Although in theory the presence of ozone should propagate ROS formation, it shows a lower concentration when combined with candles and incense compared to base cases. It does show higher concentrations when paired with frying, but still a much lower concentration than base case candles for candles + frying + ozone. It is possible, albeit a bit difficult, to relate this to particle characteristics and variability in results.

4.1.1 Effects of particle size

Particle size certainly affects the ability of the PM to bind particle-bound ROS, but it is difficult to draw conclusions on ROS concentrations solely based on particle size. The samples containing candles overall displayed high ROS concentration, while simultaneously having the largest particle sizes, which somewhat contradicts the theory that smaller particle sizes lead to increased particle-bound ROS. However, it is likely that since all particle types exist within a small enough size range (roughly 200 – 400 nm), the difference in size is simply too small to demonstrate interparticle variability. At least not on such a scale that it isn't offset by other factors.

4.1.2 Effects of metals

Metals were detected to some extent in filters of all sampled particle types. One or more key metals that exist in more than one valence form were present on all filter types. However, not all combinations were tested for metals, although as their component particle types were shown to contain metals, it is reasonable to assume that the combinations do so too. The only particle type not screened for metals at all was squalene.

The positive Spearman correlation coefficient for ROS concentration and total metal concentration supports the theory that the presence of metals propagates ROS formation. As for individual metals, iron and nickel are suggested to have the strongest positive correlation to ROS concentration, whereas copper and lead are suggested to have a negative correlation. However, there are sources of uncertainties to drawing conclusions from this, such as CFS samples consistently falling below limit of detection for metals, and large spans of standard deviation. Further testing would help deduce the statistical significance of these results.

4.1.3 Effects of ozone and SOA formation

Of the experiments that involved added ozone, such as candles + ozone and frying + ozone, only frying + ozone exhibited higher ROS concentrations than the base case. Notable ROS concentrations were detected in the squalene-ozone experiments, as in the (to a lesser extent) SOA experiments. These findings are supported by the theory of ozone interactions with VOCs and skin oil, as described in 1.1.3, that exacerbate ROS production.

However, the reverse relationship was exhibited by experiments involving candles and incense. This is caused by probe scavenging/adsorption on the black carbon present in these samples. This highlights the complexity of interpreting ROS data in mixed samples.

4.1.4 Variability between experiments and implications for interpretation

One of the most eye-catching results from the traditional method was the large variability in ROS concentration between individual experiments of the same particle type. In some cases, these differences were in magnitudes several times between experiments. This could be because of heterogeneity in particle generation despite the standardized setup of the experiments. A larger dataset would help discern if this is the case, or if it is because of some other unknown factor.

It is also possible that some type of systematic bias in the operating procedure is behind the variability. It was observed that when sonicating the vials to create the stock solutions not all the visible particle residue, particularly those containing black carbon, on the vial walls would integrate with the suspension. This could lead to underestimating particle concentration in the stock solution, an assumption that affects the interpretation of ROS concentration.

4.1.5 Comparison to existing research

As previously stated, research on particle-bound ROS from indoor sources (particularly those used in this study) is limited, making direct comparison difficult. One study that looked at OP from some indoor sources identified incense as a relatively impactful source of OP, greater than that of scented candles used in the same study (Hu et al., 2023). Assuming methodology is comparable (e.g. burning time of incense during experiment phase, scented candle is comparable to tapered candle), this is interesting because the results in this thesis show that candles are a greater source of particle-bound ROS than incense. This exemplifies that one method or probe is insufficient to determine total ROS contributions of a sample. Particles from one source could carry little particle-bound ROS but generate high levels of oxidative stress in cells through OP, meaning that conclusions on toxicity based on one or the other could paint different pictures.

A different study looked at the relation between generation of particle-bound ROS from alpha-pinene in the presence of ozone and nitric oxide (NO) (Liu & Hopke, 2014). It found that higher concentrations of ozone led to more generated ROS, but also that NO (which could be introduced in the indoor environment through e.g. quickly scavenged ozone to form nitrous oxide (NO_2). At double the concentration of NO compared to ozone, no ROS were formed at all. This indicates that the reality of indoor air composition is a complex thing and is not always fairly replicated in laboratory environments. How likely the conditions of the alpha-pinene experiments in this thesis (presence of ozone but no NO_2 or other scavenging agent) are to be met in reality is not explored further, but does provide a point of interest.

A study on oxidative potential of logwood and pellet burning found that “bad” burning conditions, such as low combustion temperature and decreased air flow

increased the number and mass concentration of aerosol particles and ROS concentration (Miljevic & Heringa et al., 2010). This has implications for other combustion and black carbon producing processes, such as the burning of candles included in this thesis. In the experimental setup, “bad” burning conditions were encouraged by having a fan constantly blow on the flame to cause flickering, which promotes soot formation and incomplete combustion. While “good” burning conditions such as no flickering and stable access to air was not studied, it could be assumed that the ROS concentration detected from candles would be lower. This could be of interest for further study.

A study on VOCs from endogenous metabolic activity and microbial transformation of sweat and sebum found that skin-relevant VOCs induce intracellular ROS (Finnegan et al., 2025). In particular, nonanal, decanal, and acetic acid gave rise to significant OP. This further highlights skin-oils and bioeffluents, such as the squalene studied in this thesis, as a source of indoor aerosol ROS.

4.2 Analysis of PINQ results and comparison with traditional method

A central motivation for this thesis was to evaluate the comparability of real-time ROS measurements using PINQ with traditional offline DCFH-based results.

Five particle types, when analyzed in PINQ, exhibit negative fluorescence. This is likely caused by scavenging and negative feedback from the presence of black carbon in these samples. However, some of the particle types that contain black carbon still exhibit positive fluorescence, notably candles + SOA and candles + frying + SOA. This suggests that SOA counteracts or is less receptive to the effects of scavenging.

It is difficult to compare the results from PINQ with the traditional method. For one, the use of different probes (BPEAnit in PINQ, DCFH in traditional) means that they are sensitive to different ranges of ROS. One probe might be missing ROS that the other probe is able to pick up, and vice versa. While a positive correlation is expected between the methods, the negative Spearman and Pearson correlation coefficients in figure 17 suggest a negative correlation instead. However, this is in large part due to the scavenging of the probe from the black carbon samples leading to negative results in the PINQ.

Originally, it was intended to use the BPEAnit probe also during the traditional method stage, as it was the probe used for the PINQ experiments and would therefore allow for more direct comparison. However, during trial runs, it exhibited characteristics such as incoherent results that suggested it was not suitable for the traditional method operating procedure. Second, the traditional method only measured ROS after several hours, once the samples had aged and given ample time

to react with the probe, while PINQ measurements occurred instantly. Exactly how this affects observed ROS concentration is difficult to ascertain, but one gives an overlook over time while the other only provides a snapshot. Observing only the PINQ results that show positive ROS concentration, the relative order of magnitude between particle types do not coincide with those shown by the traditional method.

While the traditional method successfully detected ROS across all particle types, it is subject to several limitations, including long delays between sampling and analysis and potential losses of short-lived ROS. The PINQ offers advantages in temporal resolution and can detect the short-lived ROS that traditional methods miss. Discrepancies between the two methods could indicate methodological failure but should rather be viewed as differences in chemical sensitivity and measurement artefacts.

These results indicate that no single assay can fully characterize the oxidative properties of PM. Instead, complementary use of multiple probes and methods may be necessary to obtain a more complete picture of particle-bound ROS. The use of one method over the other should be dependent on what factors are prioritized by the user.

4.3 Implications for indoor air quality and health relevance

Given that people spend the majority of their time indoors, the detection of ROS levels from common household activities such as candle burning, incense use, cooking-related processes and even bioeffluents is of clear public health relevance. Deciding limits of safe exposure is outside the scope of this thesis, but the findings help deepen the understanding of what indoor air is composed of. Furthermore, real-time monitoring techniques such as PINQ may play an important role in identifying short-term exposure events that are not captured by conventional PM mass measurements.

4.4 Limitations and future work

Several limitations should be acknowledged, aside from those previously mentioned. The number of experiments per particle type was limited, as was the number of vials per experiment analyzed by the traditional method. Not all particle types were characterized for metals, although the reasoning behind this decision was that it would be superfluous. Extraction efficiency and probe interactions introduce additional uncertainty, particularly for black carbon-rich samples. Furthermore, the

lack of direct, quantitative comparison between PINQ and DCFH results limits conclusions regarding comparison between methods.

Another factor that posed an immediate problem during the extraction phase was that the vials used to contain the particles displayed a significant natural variation in mass. This is illustrated in figure 18 showing a large subset of total mass measurements of one of the reference vials. Although the exact reason for this is unknown, it could be because of adsorption of moisture or particles on the outside of the vials, or electrostatic interference with the scales. Of 37 instances of weighing the vial where the ambient temperature was observed at the same time, the Spearman correlation coefficient for mass and temperature was 0.9184. This suggests a strong positive correlation between mass and temperature, meaning that a climate controlled environment could produce more even results.

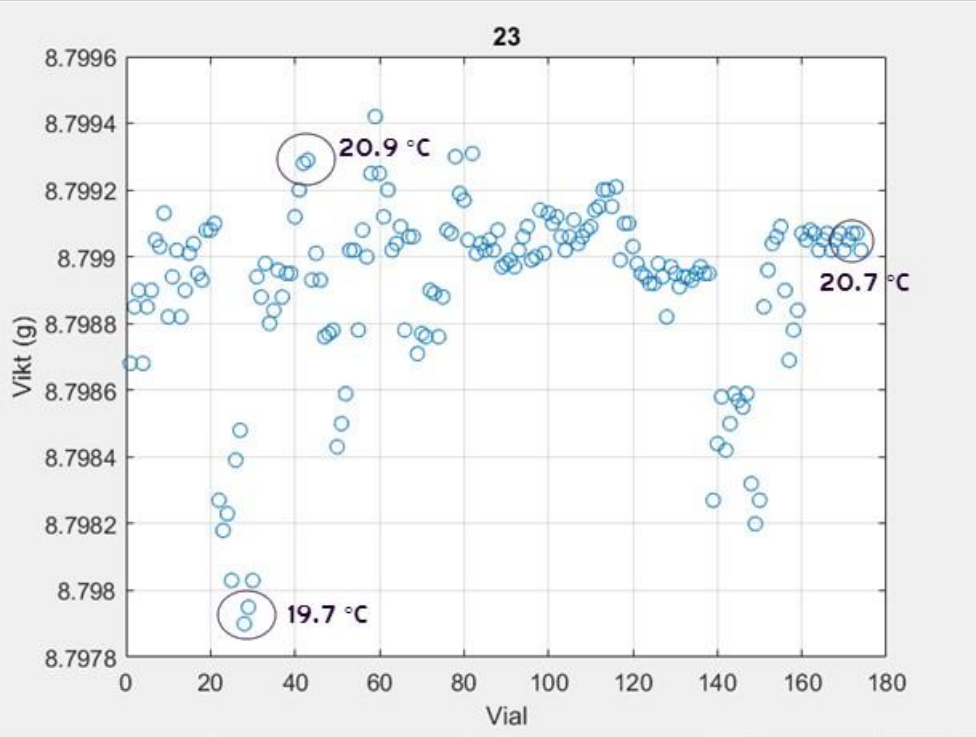

Figure 19: Variability in mass of reference vial "23"

As the mass of the vials directly affects the assumed mass of particles, such discrepancies are potentially magnified during the analysis phase. The average correction for extracted particles was 0,95 mg (in either direction). For reference, the mass of particles extracted from the filters was determined to be between 0.4 and 3.0 mg. Such a discrepancy would therefore have significant impact on the results. Since this was only discovered partway through the extraction process, it

was not possible to fully correct for this but was addressed using proxies for concerned vials.

Future work should focus on increasing experimental replication and eliminating unnecessary factors of uncertainty such as vial mass. Additionally, applying multiple ROS probes in parallel, and further investigating probe-particle interactions, particularly for black carbon-rich aerosols is also of interest.

5 References

Alessandro, C., Romano, M. P., Lionetto, M. G., Contini, D., & Guascito, M. R. (2023). An Overview of the Automated and On-Line Systems to Assess the Oxidative Potential of Particulate Matter. *Atmosphere, 14*(256). doi:https://doi.org/10.3390/

Bates, J. T., Fang, T., Verma, V., Zeng, L., Weber, R. J., Tolbert, P. E., . . . Russell, A. G. (2019). Review of Acellular Assays of Ambient Particulate Matter Oxidative Potential: Methods and Relationships with Composition, Sources, and Health Effects. *Environmental Science & Technology, 53*, 4003−4019. doi:10.1021/acs.est.8b03430

Bates, J. T., Weber, R. J., Abrams, J., Verma, V., Fang, T., Klein, M., . . . Russell, A. G. (2015). Reactive Oxygen Species Generation Linked to Sources of Atmospheric Particulate Matter and Cardiorespiratory Effects. *Environmental Science & Technology, 49*(22), 13605–13612. doi:https://doi.org/10.1021/acs.est.5b02967

Utinger B., Barth, A., Paul, A., Mukherjee, A., Campbell, S. J., Christa-Maria Müller, Ihalainen, M., Pasi Yli-Pirilä, Miika Kortelainen, Fang, Z., Mertens, P., Somero, M., Juho Louhisalmi, Thorsten Hohaus, Czech, H., Olli Sippula, Rudich, Y., Zimmermann, R., & Kalberer, M. (2024). *Emission dynamics of reactive oxygen species and oxidative potential in particles from a gasoline car and wood stove*. https://doi.org/10.5194/ar-2024-27

Brown, R. A., Stevanovic, S., Bottle, S., & Ristovski, Z. D. (2019). An instrument for the rapid quantification of PM-bound ROS: the Particle Into Nitroxide Quencher (PINQ). *Atmospheric Measurement Techniques*, *12*(4), 2387–2401. https://doi.org/10.5194/amt-12-2387-2019

Carlino, A., Maria Pia Romano, Maria Giulia Lionetto, Contini, D., & Maria Rachele Guascito. (2023). An Overview of the Automated and On-Line Systems to Assess the Oxidative Potential of Particulate Matter. *Atmosphere*, *14*(2), 256–256. https://doi.org/10.3390/atmos14020256

Chen, X., Zhong, Z., Xu, Z., Chen, L., & Wang, Y. (2010). 2′,7′-Dichlorodihydrofluorescein as a fluorescent probe for reactive oxygen species measurement: Forty years of application and controversy. *Free*

Radical Research, *44*(6), 587–604. https://doi.org/10.3109/10715761003709802Chow, J. C., Watson, J. G., Mauderly, J. L., Costa, D. L., Wyzga, R. E., Vedal, S., . . . Dockery, D. W. (2006). Health effects of fine particulate air pollution: lines that connect. *Journal of the Air & Waste Management Association, 56*(6), 709-42. doi:10.1080/10473289.2006.10464485

Chuang, H.-C., Jones, T. P., Lung, S.-C. C., & BéruBé, K. A. (2011). Soot-driven reactive oxygen species formation from incense burning. *Science of the Total Environment*, *409*(22), 4781–4787. https://doi.org/10.1016/j.scitotenv.2011.07.041

Coffaro, B., & Weisel, C. P. (2022). Reactions and Products of Squalene and Ozone: A Review. *Environmental Science & Technology*, *56*(12), 7396–7411. https://doi.org/10.1021/acs.est.1c07611

Daher, N., Ning, Z., Cho, A. K., Shafer, M., Schauer, J. J., & Sioutas, C. (2011). Comparison of the Chemical and Oxidative Characteristics of Particulate Matter (PM) Collected by Different Methods: Filters, Impactors, and BioSamplers. *Aerosol Science and Technology*, *45*(11), 1294–1304.

Directive 2008/50/EC. *Directive 2008/50/EC of the European Parliament and of the Council of 21 May 2008 on ambient air quality and cleaner air for Europe.* https://eur-lex.europa.eu/eli/dir/2008/50/oj/eng

Finnegan, M., Bolikava, V., Walsh, N., & Morrin, A. (2025). Skin-derived volatile organic compounds trigger redox signalling pathways in human keratinocytes via gas-phase interaction. RSC Advances, 15(39), 32768–32777. https://doi.org/10.1039/d5ra02839f

Ghio, A. J., Carraway, M. S., & Madden, M. C. (2012). Composition of Air Pollution Particles and Oxidative Stress in Cells, Tissues, and Living Systems. *Journal of Toxicology and Environmental Health, Part B*, *15*(1), 1–21. https://doi.org/10.1080/10937404.2012.632359

Hu, H., Ye, J., Liu, C., Yan, L., Yang, F., & Qian, H. (2023). Emission and oxidative potential of PM2.5 generated by nine indoor sources. *Building and Environment*, *230*, 110021. https://doi.org/10.1016/j.buildenv.2023.110021

Hung, H.-F., & Wang, C.-S. (2001). Experimental determination of reactive oxygen species in Taipei aerosols. *Journal of Aerosol Science*, *32*(10), 1201–1211. https://doi.org/10.1016/S0021-8502(01)00051-9

Jovanovic, M. V., Savic, J. Z., Salimi, F., Stevanovic, S., Brown, R. A., Milena Jovasevic-Stojanovic, Manojlovic, D., Bartonova, A., Bottle, S., & Ristovski, Z. D. (2019). Measurements of Oxidative Potential of Particulate Matter at Belgrade Tunnel; Comparison of BPEAnit, DTT and DCFH

Assays. *International Journal of Environmental Research and Public Health*, *16*(24), 4906–4906. https://doi.org/10.3390/ijerph16244906

Kim, H., & Xue, X. (2020). Detection of Total Reactive Oxygen Species in Adherent Cells by 2',7'-Dichlorodihydrofluorescein Diacetate Staining. Journal of Visualized Experiments, 160. https://doi.org/10.3791/60682Li, S., Liu, D., Hu, D., Kong, S., Wu, Y., Ding, S., Cheng, Y., Qiu, H., Zheng, S., Yan, Q., Zheng, H., Hu, K., Zhang, J., Zhao, D., Liu, Q., Sheng, J., Ye, J., He, H., & Ding, D. (2021). Evolution of Organic Aerosol From Wood Smoke Influenced by Burning Phase and Solar Radiation. *Journal of Geophysical Research: Atmospheres*, *126*(8). https://doi.org/10.1029/2021jd034534

Li, Y. R., & Trush, M. (2016). Defining ROS in Biology and Medicine. Reactive Oxygen Species, 1(1). https://doi.org/10.20455/ros.2016.803

Liu, Y., & Hopke, P. K. (2014). A chamber study of secondary organic aerosol formed by ozonolysis of α-pinene in the presence of nitric oxide. *Journal of Atmospheric Chemistry*, *71*(1), 21–32. https://doi.org/10.1007/s10874-014-9278-9

Lu, L., Ng, V. Y. Z., Tan, M. Z. H., Kasthuriarachchi, N. Y., Laura-Helena Rivellini, Tan, Y. Q., Ang, L., Viera, M., Bay, B. H., Seow, W. J., & Lee, A. K. Y. (2023). Particle-bound reactive oxygen species in cooking emissions: Aging effects and cytotoxicity. *Atmospheric Environment*, *319*, 120309–120309. https://doi.org/10.1016/j.atmosenv.2023.120309

Malmborg, V., Elam, D. A., Battista, V. D., Rissler, J., Clausen, P. A., Vogel, U., Wohlleben, W., & Jacobsen, N. R. (2025). Toxicity of Carbon Nanomaterials: A model to predict ROS production from easily measurable surface characteristics. *Carbon*, 119997–119997. https://doi.org/10.1016/j.carbon.2025.119997

Matz, C., Stieb, D., Davis, K., Egyed, M., Rose, A., Chou, B., & Brion, O. (2014). Effects of Age, Season, Gender and Urban-Rural Status on Time-Activity: Canadian Human Activity Pattern Survey 2 (CHAPS 2). *International Journal of Environmental Research and Public Health*, *11*(2), 2108–2124. https://doi.org/10.3390/ijerph110202108

Montesinos, V. N., Sleiman, M., Cohn, S., Litter, M. I., & Destaillats, H. (2015). Detection and quantification of reactive oxygen species (ROS) in indoor air. *Talanta*, *138*, 20–27. https://doi.org/10.1016/j.talanta.2015.02.015

Miljevic, B., Fairfull-Smith, K. E., Bottle, S. E., & Ristovski, Z. D. (2010). The application of profluorescent nitroxides to detect reactive oxygen species derived from combustion-generated particulate matter: Cigarette smoke – A case study. *Atmospheric Environment*, *44*(18), 2224–2230. https://doi.org/10.1016/j.atmosenv.2010.02.043

Miljevic, B., Heringa, M. F., Keller, A., Meyer, N. K., Good, J., Lauber, A., DeCarlo, P. F., Fairfull-Smith, K. E., Nussbaumer, T., Burtscher, H., Prevot, A. S. H., Baltensperger, U., Bottle, S. E., & Ristovski, Z. D. (2010). Oxidative Potential of Logwood and Pellet Burning Particles Assessed by a Novel Profluorescent Nitroxide Probe. Environmental Science & Technology, 44(17), 6601–6607. https://doi.org/10.1021/es100963y

Mudway, I. S., Stenfors, N., Duggan, S. T., Roxborough, H., Zielinski, H., Marklund, S. L., Blomberg, A., Frew, A. J., Sandström, T., & Kelly, F. J. (2004). An in vitro and in vivo investigation of the effects of diesel exhaust on human airway lining fluid antioxidants. *Archives of Biochemistry and Biophysics*, *423*(1), 200–212. https://doi.org/10.1016/j.abb.2003.12.018

Murr, L. (2008). Cytotoxicity and reactive oxygen species generation from aggregated carbon and carbonaceous nanoparticulate materials. *International Journal of Nanomedicine*, 83. https://doi.org/10.2147/ijn.s2464

Nel, A. (2006). Toxic Potential of Materials at the Nanolevel. *Science*, *311*(5761), 622–627. https://doi.org/10.1126/science.1114397

Oberdörster, G., Oberdörster, E., & Oberdörster, J. (2005). Nanotoxicology: An Emerging Discipline Evolving from Studies of Ultrafine Particles. *Environmental Health Perspectives*, *113*(7), 823–839. https://doi.org/10.1289/ehp.7339

Pritchard, R. J., Ghio, A. J., Lehmann, J. R., Winsett, D. W., Tepper, J. S., Park, P., M. Ian Gilmour, Dreher, K. L., & Costa, D. L. (1996). Oxidant Generation and Lung Injury after Particulate Air Pollutant Exposure Increase with the Concentrations of Associated Metals. *Inhalation Toxicology*, *8*(5), 457–477. https://doi.org/10.3109/08958379609005440

Prolo, C., Ríos, N., PiacenzaL., María Noel Álvarez, & Radí, R. (2018). Fluorescence and chemiluminescence approaches for peroxynitrite detection. *Free Radical Biology and Medicine*, *128*, 59–68. https://doi.org/10.1016/j.freeradbiomed.2018.02.017

Puthussery, J. V., Singh, A., Rai, P., Bhattu, D., Kumar, V., Vats, P., Furger, M., Rastogi, N., Slowik, J. G., Ganguly, D., Prevot, A. S. H., Tripathi, S. N., & Verma, V. (2020). Real-Time Measurements of $PM_{2.5}$ Oxidative Potential Using a Dithiothreitol Assay in Delhi, India. *Environmental Science & Technology Letters*, *7*(7), 504–510. https://doi.org/10.1021/acs.estlett.0c00342

Ristovski, Z. D., Bottle, S., Stevanovic, S., & Brown, R. A. (2019). An instrument for the rapid quantification of PM-bound ROS: the Particle Into Nitroxide Quencher (PINQ). *Atmospheric Measurement Techniques, 12*, 2387–2401,. doi:https://doi.org/10.5194/amt-12-2387-2019

Schweizer, C., Edwards, R. D., Bayer-Oglesby, L., Gauderman, W. J., Ilacqua, V., Juhani Jantunen, M., Lai, H. K., Nieuwenhuijsen, M., & Künzli, N. (2006). Indoor time–microenvironment–activity patterns in seven regions of Europe. *Journal of Exposure Science & Environmental Epidemiology*, *17*(2), 170–181. https://doi.org/10.1038/sj.jes.7500490

Shu, Z., Huang, C., Min, K., Long, C., Liu, L., Tan, J., Liu, Q., & Jiang, G. (2023). Analysis of black carbon in environmental and biological media: Recent progresses and challenges. TrAC Trends in Analytical Chemistry, 169, 117347. https://doi.org/10.1016/j.trac.2023.117347

Stevanovic, S., Vaughan, A., Hedayat, F., Salimi, F., Rahman, M. M., Zare, A., Brown, R. A., Brown, R. J., Wang, H., Zhang, Z., Wang, X., Bottle, S. E., Yang, I. A., & Ristovski, Z. D. (2017). Oxidative potential of gas phase combustion emissions - An underestimated and potentially harmful component of air pollution from combustion processes. *Atmospheric Environment*, *158*, 227–235. https://doi.org/10.1016/j.atmosenv.2017.03.041

Strak, M., Janssen, N. A., Godri, K. J., Gosens, I., Mudway, I. S., Cassee, F. R., . . . Hoek, G. (2012). Respiratory health effects of airborne particulate matter: the role of particle size, composition, and oxidative potential-the RAPTES project. *Environmental Health Perspectives, 120*(8), 1183-9. doi:10.1289/ehp.1104389

Tong, H., Jeanne, S., Arangio, A. M., Socorro, J., Shen, F., Lucas, K., Brune, W. H., Ulrich Pöschl, & Manabu Shiraiwa. (2018). Reactive Oxygen Species Formed by Secondary Organic Aerosols in Water and Surrogate Lung Fluid. *Environmental Science & Technology*. https://doi.org/10.1021/acs.est.8b03695

Venkatachari, P., Hopke, P. K., Grover, B. D., & Eatough, D. J. (2005). Measurement of Particle-Bound Reactive Oxygen Species in Rubidoux Aerosols. *Journal of Atmospheric Chemistry*, *50*(1), 49–58. https://doi.org/10.1007/s10874-005-1662-z

Venkatachari, P., & Hopke, P. K. (2008). Development and Laboratory Testing of an Automated Monitor for the Measurement of Atmospheric Particle-Bound Reactive Oxygen Species (ROS). *Aerosol Science and Technology*, *42*(8), 629–635. https://doi.org/10.1080/02786820802227345

Wang, R., Li, J., Wang, H., Deng, S., He, C., Miljevic, B., Ristovski, Z., & Wang, B. (2025). Development and Validation of the Particle into Nitroxide Quencher System with BPEAnit Probe for High-Sensitivity Reactive Oxygen Species Detection in Atmospheric Monitoring. *Sensors*, *25*(4), 1129. https://doi.org/10.3390/s25041129

World Health Organization. (2024). *Sustainable Development Goal indicator 3.9.1: mortality attributed to air pollution.* Geneva: World Health Organization.

Yao, K., Wang, S., Zheng, H., Zhang, X., Wang, Y., Chi, Z., & Guo, H. (2023). Oxidative potential and source apportionment of size-resolved particles from indoor environments: Dithiothreitol (DTT) consumption and ROS production. *Atmospheric Environment*, *313*, 120060. https://doi.org/10.1016/j.atmosenv.2023.120060